

Synthesis and Spectroscopic Properties of $\text{GdAl}_3(\text{BO}_3)_4$ Poly-crystals Codoped with Yb^{3+} and Eu^{3+}

C. H. Yang · G. F. Yang · Y. X. Pan · Q. Y. Zhang

Received: 7 April 2008 / Accepted: 21 May 2008 / Published online: 2 July 2008
© Springer Science + Business Media, LLC 2008

Abstract $\text{GdAl}_3(\text{BO}_3)_4$ polycrystals co-doped with Yb^{3+} and Eu^{3+} has been synthesised by combustion method with urea. Upon the excitation at 465 nm ($\text{Eu}^{3+}/^7\text{F}_6 \rightarrow ^5\text{D}_2$ transition), emission bands centered at 590, 613, 697 and 702 nm in the wavelength region of 550–750 nm have clearly been observed, assigned to the electronic transitions of $^5\text{D}_0 \rightarrow ^7\text{F}_J$ ($J=1, 2, 4$ and 5) of Eu^{3+} ions, respectively. Meanwhile, an intense emission centred at 980 nm along with a shoulder at 1,040 nm has also been observed by exploiting a cross-relaxation process between the transitions of $\text{Eu}^{3+}/^5\text{D}_0 \rightarrow ^7\text{F}_6$ and $\text{Yb}^{3+}/^2\text{F}_{7/2} \rightarrow ^2\text{F}_{5/2}$. On the contrary, an intense red up-conversion emission centred at 613 nm originated from the $^5\text{D}_0 \rightarrow ^7\text{F}_2$ transition of Eu^{3+} has been observed upon excitation with 980 nm laser diode. The quadratic dependence of the red up-conversion intensity on the pump-laser power reveals a cooperative energy transfer mechanism from a pair of Yb^{3+} ions to one Eu^{3+} ion.

Keywords Phosphor · Luminescence · Structure · Rare-earth

Introduction

Over the past several years, rare-earth (RE) doped frequency up-conversion nanocrystals have attracted great interest, for

their potential application in bio-probe, high-density optical storage, solid-state color and three-dimensional (3D) displays, and diode-pumped visible optical lasers [1–4]. Borate-based materials have been proved to be a promising host for up-conversion fluorescence, not only because of their high nonlinear optical coefficient and exceptional optical damage thresholds, but also because of their good thermal and chemical durability. Especially, $\text{RM}_3(\text{BO}_3)_4$ is a remarkable up-conversion community which are mostly derivatives of the huntite structure type with more non-centrosymmetric structures than other borates, for it has a favorable anionic groups that could able to produce higher nonlinearities and a suitable birefringence [5]. It is reported that $\text{RAl}_3(\text{BO}_3)_4$ ($R=\text{Gd}, \text{Y}, \text{Nd}$) crystals doped with various RE ions such as Yb^{3+} , Nd^{3+} , Er^{3+} , Dy^{3+} , etc. have shown excellent self-frequency up-conversion properties as diode-pumped laser [6–10].

Herein, the main objective of this work is to carry out a detailed study on the synthesis, structural and spectral properties of $\text{GdAl}_3(\text{BO}_3)_4$ polycrystals co-doped with Yb^{3+} and Eu^{3+} by using a combustion method, to examine their suitability as potential phosphors in bio-probe, diode-pumped visible optical lasers and photonic applications. Near-infrared (NIR) luminescence at 980 nm under the visible excitation as well as the intense red up-conversion emission centred at 613 nm upon the excitation with 980 nm laser diode (LD) has been observed, the possible energy transfer mechanisms involved have been systematically investigated and discussed.

Experiments

$\text{Gd}_{1-x-y}\text{Al}_3(\text{BO}_3)_4/\text{Eu}_y\text{Yb}_x$ ($x=0, 0.01, 0.1, 0.2, 0.5, 0.75$ mol%, $y=0.01\sim 0.02$ mol%) powders were synthesised

C. H. Yang · G. F. Yang · Q. Y. Zhang (✉)
MOE Key Lab of Specially Functional Materials,
South China University of Technology,
Guangzhou 510640, People's Republic of China
e-mail: qyzhang@scut.edu.cn

Y. X. Pan
College of Chemistry, South China University of Technology,
Guangzhou 510640, People's Republic of China

by combustion method with urea as fuel [11, 12]. Gd_2O_3 (99.99%), Yb_2O_3 (99.99%), Eu_2O_3 (99.99%), H_3BO_3 (A.R.), $\text{Al}(\text{NO}_3)_3 \cdot 9\text{H}_2\text{O}$ (A.R.), nitric acid (A.R.), urea (A.R.) were used as raw materials. All the RE oxides were first dissolved with nitric acid, and then their nitrate solutions were mixed together in stoichiometric proportion with 5 mol% excess of H_3BO_3 . Subsequently, urea was added into the solutions with a molar ratio of metal ions/urea=1:3. After evaporating and burning, the precursors were sintered in hot active carbon atmosphere at 980 °C for 10 h to complete the crystallization.

The crystal structures were analyzed by a Philips PW1830 X-ray powder diffractometer (XRD) with Cu K α radiation ($\lambda=1.5406$ Å). A scanning electron microscopy (SEM) (JEOL JSM-6340F) operated at 5 kV was used to characterize the size and morphology of the synthesized $\text{GdAl}_3(\text{BO}_3)_4$ phosphors. The up-conversion spectra of $\text{Yb}^{3+}/\text{Eu}^{3+}$ co-doped $\text{GdAl}_3(\text{BO}_3)_4$ phosphors were obtained on a TRIAX320 spectrofluorimeter (Jobin-Yvon Inc., Longjumeau, France) with Hamamatsu R928 photomultiplier tube (PMT) (Hamamatsu Co., Japan) under the excitation of 980 nm laser diode (Coherent Co. USA). During the detection, a Scog HWB780 nm cutoff filter (Ygyes Co., China) was used in combination with the 980 nm LD. The normal excitation and NIR emission spectra had been recorded using a 450-W xenon lamp as the excitation source. Emitted light was focused on to the monochromator and was monitored at the exit slit by a photon-counting R5108 PMT (Hamamatsu Co., Japan). The emissions around 1 μm were obtained using a Scog HB550 nm filter (Ygyes Co., China) in combination with the detector. Decay lifetimes of $\text{Eu}^{3+}/^5\text{D}_0$ under the excitation of a Spex flash lamp were recorded using a digital storage oscillograph (model TDS 3012B, Tektronix Co., Beaverton, OR, USA) controlled by a personal computer.

Results and discussion

Structural properties of $\text{GdAl}_3(\text{BO}_3)_4$ phosphor

Figure 1 shows the experimental X-ray diffraction profile for RE-doped $\text{GdAl}_3(\text{BO}_3)_4$ white powder samples. All the diffraction peaks agree well with the pure hexagonal $\text{GdAl}_3(\text{BO}_3)_4$ with huntite structure (JCPDS card of 38-1248). The cell parameters of $\text{GdAl}_3(\text{BO}_3)_4$ are $a=0.9302$ nm, $c=0.7259$ nm, and the space group is R32. The $\text{GdAl}_3(\text{BO}_3)_4$ crystal is hexagonal phase and isostructural with huntite $\text{CaMg}_3(\text{CO}_3)_4$ [13], the doped ion has replaced Gd^{3+} ion site in this host [13, 14]. A typical SEM images of $\text{GdAl}_3(\text{BO}_3)_4$ powder phosphors is shown in the inset of Fig. 1. The average size of the polycrystal phosphors is about 0.4 μm .

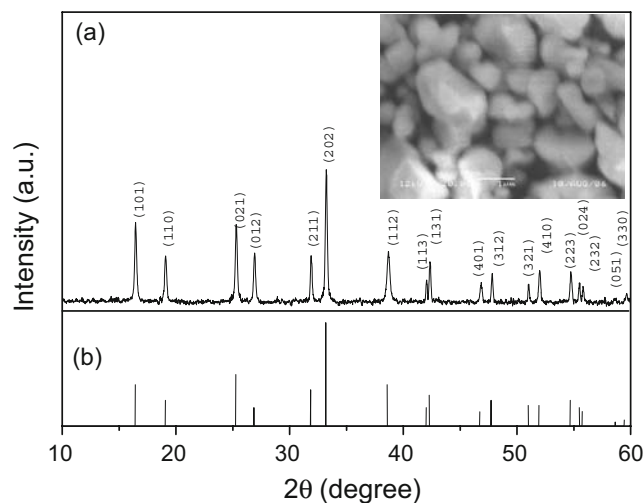


Fig. 1 X-ray diffraction pattern of the prepared rare-earth doped $\text{GdAl}_3(\text{BO}_3)_4$ phosphor (a), accompanied with reference $\text{GdAl}_3(\text{BO}_3)_4$ (JCPDS card 38-1248) (b). Inset shows a typical SEM image of $\text{GdAl}_3(\text{BO}_3)_4$ powder phosphors

Luminescence

Figure 2 shows the excitation spectra of $\text{Gd}_{0.79}\text{Al}_3(\text{BO}_3)_4/\text{Eu}_{0.01}, \text{Yb}_{0.01}$ phosphors monitored both at 613 and 980 nm. Two main excitation bands peaked at 395 and 465 nm have been obtained in the wavelength region of 300–500 nm by monitored the 613 nm emission of Eu^{3+} , which are assigned to the transitions of Eu^{3+} ions from the ground state $^7\text{F}_0$ to the excited states $^5\text{L}_6$ and $^5\text{D}_2$, respectively. It is interesting to note that the excitation bands centred at 395 and 465 nm have also been clearly observed by monitoring the 980 nm emission of Yb^{3+} . Upon excitation with 395 and 465 nm, four visible emission bands centred at 590, 613, 697 and 702 nm of $\text{Eu}^{3+}/^5\text{D}_0 \rightarrow ^7\text{F}_j$ ($j=1, 2, 4, 5$) have clearly been observed as illustrated in Fig. 3. Meanwhile, it should be mentioned here that a broad NIR emission at 980 nm along with a shoulder at 1040 nm, originated from the transition of $\text{Yb}^{3+}/^2\text{F}_{5/2} \rightarrow ^2\text{F}_{7/2}$ has also been observed.

To optimize Yb^{3+} fluorescence intensity, we have investigated it for a series of Yb^{3+} concentration ($x=0, 1, 10, 20, 50, 75$ mol%) in $\text{Gd}_{0.99-x}\text{Al}_3(\text{BO}_3)_4/\text{Eu}_{0.01}, \text{Yb}_x$, and the plots of the fluorescence intensities of Eu^{3+} and Yb^{3+} ions versus the Yb^{3+} -doping concentration are shown in Fig. 4. For those Eu^{3+} -concentration fixed samples, the fluorescence intensity of Eu^{3+} decreases, while Yb^{3+} increases rapidly with increasing the concentration of Yb^{3+} up to 20 mol%. However, concentration quenching occurs when the Yb^{3+} -doping concentration is beyond 20 mol%. These results support the fact of the efficient energy transfer from Eu^{3+} to Yb^{3+} in the compounds. The possible schematic process responsible for the down-conversion from Eu^{3+} to Yb^{3+} is shown in Fig. 5. It is assumed that a cross-relaxation process

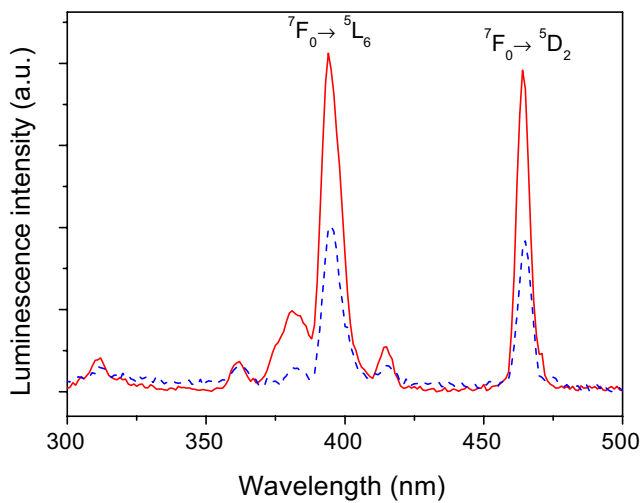


Fig. 2 Excitation spectra of the Eu^{3+} (solid line: monitored at 613 nm, and dotted line: monitored at 980 nm) in $\text{Gd}_{0.98}\text{Al}_3(\text{BO}_3)_4/\text{Eu}_{0.01}, \text{Yb}_{0.01}$ phosphor

between the levels of $\text{Eu}^{3+}/^5\text{D}_0 \rightarrow ^7\text{F}_6$ and the levels of $\text{Yb}^{3+}/^2\text{F}_{7/2} \rightarrow ^2\text{F}_{5/2}$ occurs due to the energy match [15, 16].

Figure 6 presents the dynamics of $\text{Eu}^{3+}/^5\text{D}_0 \rightarrow ^7\text{F}_2$ (613 nm) fluorescence in $\text{Eu}^{3+}/\text{Yb}^{3+}$ co-doped $\text{GdAl}_3(\text{BO}_3)_4$ phosphors excited at 465 nm. It is found that, in Eu^{3+} (1 mol%) single doped sample the Eu^{3+} emission at 613 nm in $\text{GdAl}_3(\text{BO}_3)_4$ shows as single exponential with a lifetime 1.39 ms, but when the Yb^{3+} ions are co-doped into the samples, the decay curves become non-exponential and the lifetimes decrease. The details of the decreasing lifetime of Eu^{3+} (at 613 nm) versus Yb^{3+} -doping concentration are shown in the inset of Fig. 6. These shortened decay times are consistent with the fact that the time-averaged intrinsic emission intensities decreases with Yb^{3+} concentration. Taking into account the existence of the energy migration

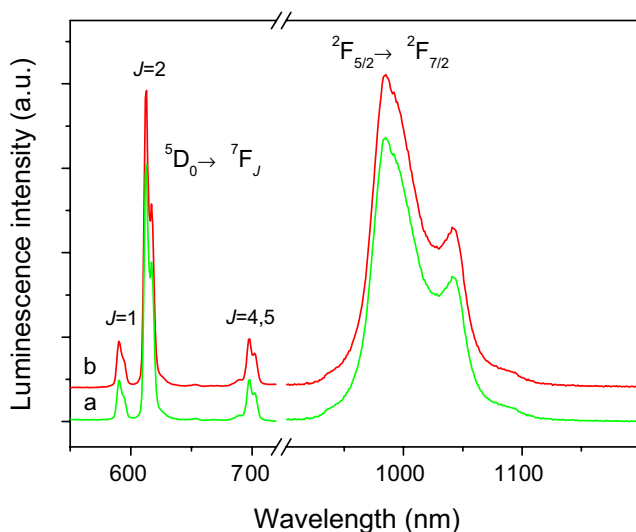


Fig. 3 Emission spectra of Yb^{3+} and Eu^{3+} in $\text{Gd}_{0.98}\text{Al}_3(\text{BO}_3)_4/\text{Eu}_{0.01}, \text{Yb}_{0.01}$ phosphor (a, excited at 465 nm; b, excited at 395 nm)

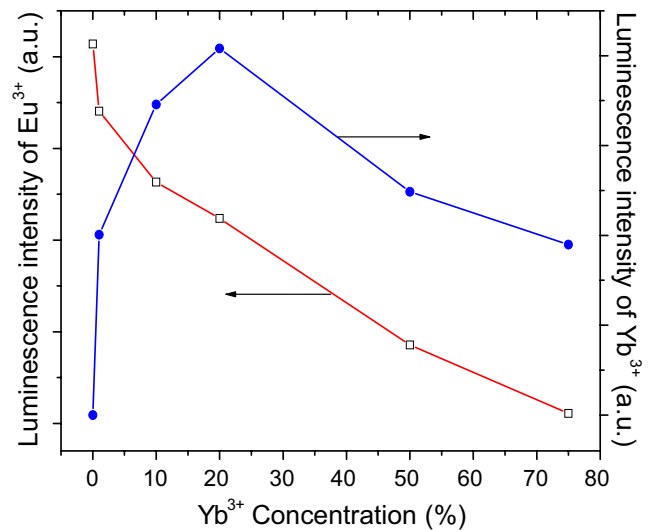


Fig. 4 The normal visible luminescence intensities Eu^{3+} and infrared fluorescence intensities Yb^{3+} versus the concentration of Yb^{3+} in $\text{Gd}_{0.99-x}\text{Al}_3(\text{BO}_3)_4/\text{Eu}_{0.01}, \text{Yb}_x$ ($x=0, 1, 10, 20, 50, 75$ mol%) phosphors

from the donor to the acceptor, the Yokota–Tanimoto model [17–20] has been used to fit the Eu^{3+} decay curves: $I(t) = I(0) \exp\left(-\frac{t}{\tau_0} - \gamma\sqrt{t} - Wt\right)$ where τ_0 is the intrinsic lifetime of donor ions, γ characterizes the direct $\text{Eu}^{3+} \rightarrow \text{Yb}^{3+}$ energy transfer, and W denotes the migration parameter. In the case of dipole–dipole interaction, γ given by the expression, $\gamma = \frac{4}{3}\pi^{3/2}N_{\text{Eu}}C_{\text{DA}}^{1/2}$, where N_{Eu} is the acceptors concentration and $C_{\text{DA}}^{(S)}$ is the donor–acceptor energy transfer micro-parameter. The best fitting is obtained from Eu^{3+} to Yb^{3+} in the $\text{Gd}_{0.99}\text{Al}_3(\text{BO}_3)_4/\text{Yb}_{0.2}, \text{Eu}_{0.01}$ sample with the values $C_{\text{DA}}^{(6)} = 6.78 \times 10^{-40} \text{ cm}^6 \text{ s}^{-1}$, indicating dipole–dipole interaction among the Tb^{3+} and Yb^{3+} ions [17].

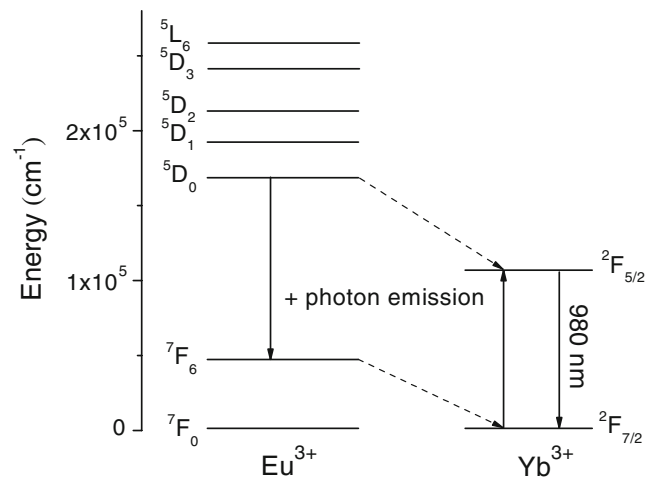


Fig. 5 The energy level of the cross-relaxation between Yb^{3+} ions and Eu^{3+} ions in $\text{Eu}^{3+}/\text{Yb}^{3+}$ co-doped $\text{GdAl}_3(\text{BO}_3)_4$ phosphors under the excitation of 465 nm

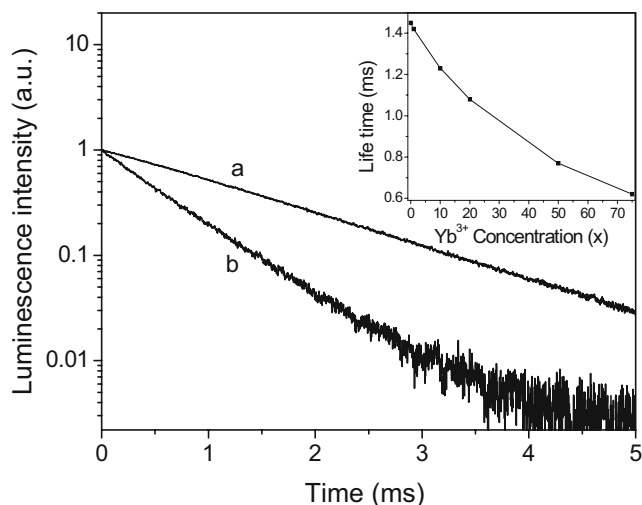


Fig. 6 Time-resolved signals of the Eu^{3+} fluorescence ($\lambda_{\text{ex}}=465$ nm, $\lambda_{\text{em}}=613$ nm) for (a) $\text{Gd}_{0.99}\text{Al}_3(\text{BO}_3)_4/\text{Eu}_{0.01}$ and (b) $\text{Gd}_{0.79}\text{Al}_3(\text{BO}_3)_4/\text{Yb}_{0.2}, \text{Eu}_{0.01}$ phosphors. The inset is the dependence of the lifetimes of the Eu^{3+} (at 613 nm) on the Yb^{3+} -doping concentration upon 465 nm excitation in $\text{Gd}_{0.99-x}\text{Al}_3(\text{BO}_3)_4/\text{Eu}_{0.01}, \text{Yb}_x$ ($x=0, 1, 10, 20, 50, 75$ mol%) phosphors

Cooperative up-conversion

Upon excitation with a 980 nm LD, intense red up-conversion emission from $\text{Eu}^{3+}/^5\text{D}_0$ in $\text{Eu}^{3+}/\text{Yb}^{3+}$ co-doped $\text{GdAl}_3(\text{BO}_3)_4$ phosphor could be easily observed by naked eyes. The visible emission bands at 590, 613, 697 and 702 nm corresponding to the multiple transitions of $\text{Eu}^{3+}/^5\text{D}_0 \rightarrow ^7\text{F}_j$ ($J=1, 2, 3$ and 5) are shown in Fig. 7. In the low-power limit, the non-linearly dependence of the up-conversion intensity I depends on the LD power P has been studied. It is typically written as

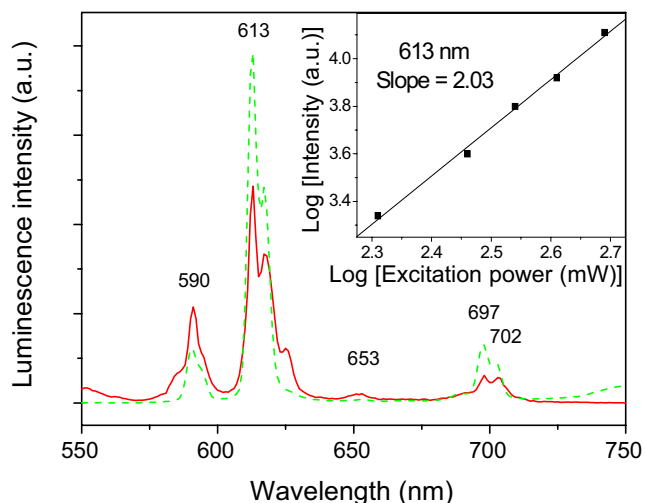


Fig. 7 Visible emission spectra of the Eu^{3+} in $\text{Gd}_{0.88}\text{Al}_3(\text{BO}_3)_4/\text{Eu}_{0.02}, \text{Yb}_{0.1}$ phosphor under the excitation of 465 nm LD (dotted line) and the normal emission spectrum of Eu^{3+} under the excitation of 980 nm (solid line) have also been recorded for comparison. The inset is the dependence of the up-conversion emission intensities on the pump power in $\text{Gd}_{0.88}\text{Al}_3(\text{BO}_3)_4/\text{Yb}_{0.1}, \text{Eu}_{0.02}$ phosphor ($\lambda_{\text{ex}}=980$ nm)

$I(P) \propto P^n$, where the $I(P)$ is the up-conversion intensity, P is the pump power, and $n=2, 3, \dots$ is the number of the pump-photons required in the up-conversion process. The inset in the Fig. 7 shows the dependence of the up-conversion emission intensities versus the pump powers for the sample with fixed Yb^{3+} (10 mol%) and Eu^{3+} (2 mol%) concentration. The red emission intensities at 613 nm have been found to be quadratic upon the excitation intensities with the obtained slope of 2.03, indicating a two-photon cooperative up-conversion process.

The energy level scheme explaining the mechanism of the cooperative up-conversion processes occurred in the $\text{Eu}^{3+}/\text{Yb}^{3+}$ co-doped $\text{GdAl}_3(\text{BO}_3)_4$ phosphors pumped by 980 nm LD is shown in Fig. 8. In the first step of the excitation process, incident NIR photons with energy in matching with the Yb^{3+} ions level gap promote them from the ground state $^2\text{F}_{7/2}$ to the excited state $^2\text{F}_{5/2}$. Then, the cooperative energy transfer process occurs via a dipole-dipole interaction from $\text{Yb}^{3+}-\text{Yb}^{3+}$ pairs to one Eu^{3+} ion and excites Eu^{3+} to the $^5\text{D}_1$ state [15, 21]. The excited state Eu^{3+} quickly relaxes to the $^5\text{D}_0$ state, from where the intense red up-conversion emissions are possible as shown in the Fig. 8.

Conclusions

In summary, we report on structural and spectral properties of $\text{GdAl}_3(\text{BO}_3)_4$ polycrystals co-doped with Yb^{3+} and Eu^{3+} by combustion method with urea. Intense emission peaked at 590, 613, 697 and 702 nm assigned to $\text{Eu}^{3+}/^5\text{D}_0 \rightarrow ^7\text{F}_j$ ($j=1, 2, 4$ and 5) have been observed under excitation with 465 nm. Meanwhile, an intense emission centred at 980 nm

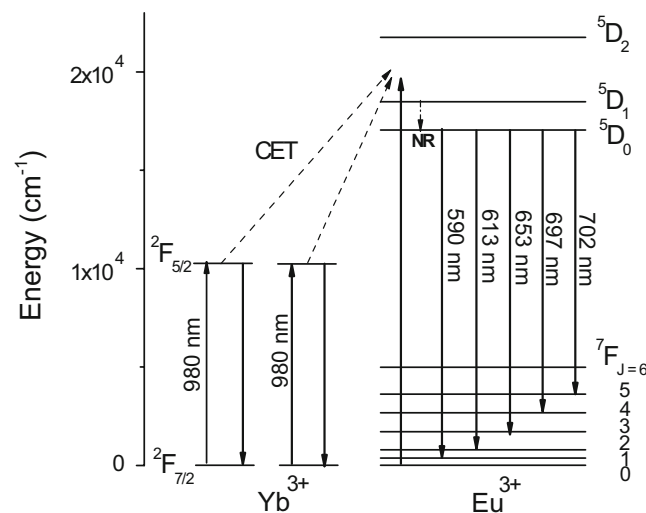


Fig. 8 The schematic diagram of cooperative energy transfer process from two Yb^{3+} ions to one Eu^{3+} ion in $\text{Gd}_{0.88}\text{Al}_3(\text{BO}_3)_4/\text{Eu}_{0.02}, \text{Yb}_{0.1}$ under the excitation of 980 nm LD

along with a shoulder at 1040 nm has also been observed by exploiting a cross-relaxation process between the transitions of $\text{Eu}^{3+}/^3\text{D}_0 \rightarrow ^7\text{F}_6$ and $\text{Yb}^{3+}/^2\text{F}_{7/2} \rightarrow ^2\text{F}_{5/2}$. On the contrary, upon excitation with 980 nm LD, an intense red up-conversion emission centred at 613 nm originated from $^5\text{D}_0 \rightarrow ^7\text{F}_2$ transition of Eu^{3+} has been obtained. The quadratic dependence of the red-emission on the pump-laser power reveals a cooperative energy transfer mechanism from a pair of Yb^{3+} ions to one Eu^{3+} ion.

References

- Maciel GS, Biswas A, Kapoor R, Prasad PN (2000) Blue cooperative upconversion in Yb^{3+} -doped multicomponent sol-gel-processed silica glass for three-dimensional display. *Appl Phys Lett* 76:1978–1980
- Yi GS, Chow GM (2005) Colloidal $\text{LaF}_3:\text{Yb,Er}$, $\text{LaF}_3:\text{Yb,Ho}$ and $\text{LaF}_3:\text{Yb,Tm}$ nanocrystals with multicolor upconversion fluorescence. *J Mater Chem* 43:4460–4464
- Zhang QY, Li T, Jiang ZH (2005) 980 nm laser-diode-excited intense blue upconversion in $\text{Tm}^{3+}/\text{Yb}^{3+}$ -codoped gallate-bismuth-lead glasses. *Appl Phys Lett* 87:171911
- Lande D, Orlov SS, Akella A, Hesselink L, Neurgaonkar RR (1997) Digital holographic storage system incorporating optical fixing. *Opt Lett* 22:1722–1724
- Becker P (1998) Borate Materials in Nonlinear Optics. *Adv Mater* 10(13):979–992
- Vázquez RM, Osellame R, Marangoni M, Ramponi R, Diéguez E, Ferrari M, Mattarelli M (2004) Optical properties of Dy^{3+} doped yttrium-aluminium borate. *J Phys-Condens Matter* 16:465–471
- Wang GF, Han TPJ, Gallagher HG, Henderson B (1995) Novel laser gain media based on Cr^{3+} -doped mixed borates $\text{RX}_3(\text{BO}_3)_4$. *Appl Phys Lett* 67:3906–3908
- Burns PA, Dawes JM, Dekker P, Piper JA, Li J, Wang JY (2002) Coupled-cavity, single-frequency, tunable cw $\text{Yb}:\text{YAB}$ yellow microchip laser. *Opt Commun* 207:315–320
- Dammak M (2005) Crystal-field analysis of Er^{3+} ions in yttrium aluminium borate (YAB) single crystals. *J Alloys Compd* 393:51–56
- Leonyuk NI, Koporulina EV, Maltsev VV, Mokhov AV, Pilipenko OV (2005) High temperature crystallization of $\text{NdAl}_3(\text{BO}_3)_4$ and $\text{YAl}_3(\text{BO}_3)_4$ doped with Sc^{3+} and Ga^{3+} . *J Cryst Growth* 281:587–591
- Yang CH, Pan YX, Zhang QY (2007) Cooperative energy transfer and frequency upconversion in $\text{Yb}^{3+}-\text{Tb}^{3+}$ and $\text{Nd}^{3+}-\text{Yb}^{3+}-\text{Tb}^{3+}$ Codoped $\text{GdAl}_3(\text{BO}_3)_4$ Phosphors. *J Fluoresc* 17: 500–504
- Pan YX, Zhang QY, Jiang ZH (2007) Comparative investigation on nanocrystal structure and luminescence properties of gadolinium molybdates codoped with $\text{Er}^{3+}/\text{Yb}^{3+}$. *J Fluoresc* 17:444–451
- Kellendonk F, Belt TD, Blasse G (1982) On the luminescence of bismuth, cerium, and chromium and yttrium aluminum borate. *J Chem Phys* 76:1194–1199
- Zhang QY, Yang GF, Jiang ZH (2007) Cooperative down-conversion in $\text{GdAl}_3(\text{BO}_3)_4:\text{RE}^{3+},\text{Yb}^{3+}$ ($\text{RE}=\text{Pr, Tb, and Tm}$). *Appl Phys Lett* 91:051903
- Stein G, Würzberg E (1975) Energy gap law in the solvent isotope effect on radiationless transitions of rare earth ions. *J Chem Phys* 62:208–213
- Jubera V, Garcia A, Chaminade JP, Guillen F, Sablayrolles J, Fouassier C (2007) Yb^{3+} and $\text{Yb}^{3+}-\text{Eu}^{3+}$ luminescent properties of the $\text{Li}_2\text{Lu}_5\text{O}_4(\text{BO}_3)_3$ phase. *J Lumin* 124:10–14
- Yokota M, Tanimoto O (1967) Effects of diffusion on energy transfer by resonance. *J Phys Soc Jpn* 22:779–783
- Burshtein AI (1972) Hopping mechanism of energy transfer. *Sov Phys JETP* 35:882–886
- Balda R, Fernández J, Iparraguirre I, Al-Saleh M (2006) Spectroscopic study of $\text{Nd}^{3+}/\text{Yb}^{3+}$ in disordered potassium bismuth molybdate laser crystals. *Opt Mater* 28:1247–1252
- Jaque D, Ramirez MO, Bausá LE, García Solé J, Cavalli E, Speghini A, Bettinelli M (2003) $\text{Nd}^{3+}-\text{Yb}^{3+}$ energy transfer in the $\text{YAl}_3(\text{BO}_3)_4$ nonlinear laser crystal. *Phys Rev B* 68:035118
- Maciel GS, Biswas A, Prasad PN (2000) Infrared-to-visible Eu^{3+} energy upconversion due to cooperative energy transfer from an Yb^{3+} ion pair in a sol-gel processed multi-component silica glass. *Opt Mater* 178:65–69